UDK 669.71:52-334.2
Original scientific article/Izvirni znanstveni članek

ISSN 1580-2949
Mater. Tehnol.

STUDY ON TIG ADDITIVE MANUFACTURING OF 4043 ALUMINIUM ALLOY

ŠTUDIJ TIG DODAJALNE TEHNOLOGIJE NA Al ZLITINI TIPA 4043

Lixing Qiu*, Yu Zhang

College of Mechanical Engineering, Shenyang University, Shenyang 110044, China

Prejem rokopisa – received: 2025-02-22; sprejem za objavo – accepted for publication: 2025-10-07

doi:10.17222/mit.2025.1403

4043 aluminum alloy components were successfully fabricated in this study using TIG (tungsten inert gas) additive manufacturing with an ER4043 filler wire. The microstructure and mechanical properties of the as-deposited material were systematically investigated. Results demonstrated that the TIG-deposited components exhibited favorable geometric integrity. Metallographic observations revealed a microstructure dominated by coarse dendritic grains, which grew continuously across interlayer regions. Tensile tests indicated minimal anisotropy in strength: the average tensile strength parallel and perpendicular to the welding direction was 146.1 MPa and 148.7 MPa, respectively. However, the elongation parallel to the welding direction (23.91 %) was notably higher than that perpendicular to it (19.31 %). The observed elongation (19–24 %) surpasses conventional cast 4043 alloys (≈10–15 %), likely due to the absence of large-scale casting defects (e.g., shrinkage cavities). This highlights the potential of TIG AM as a hybrid manufacturing method for aluminum components requiring balanced strength and ductility.

Keywords: additive manufacturing, 4043 aluminum alloy, as-deposited microstructure, mechanical properties

Avtorji v članku opisujejo izdelavo različnih komponent iz Al zlitine tipa 4043 z uporabo dodajalne tehnologije (AM; angl.: additive manufacturing) na osnovi navarjanja z stabilno volframovo elektrodo v zaščitnem plinu (TIG; angl.: Tungsten Inert Gas). Kot polnilno žico za navarjanje so uporabili žico tipa ER4043. Nato so sistematično preiskovali mikrostrukturo in določili mehanske lastnosti izdelanega materiala. Rezultati raziskav so pokazali, da imajo s TiG-AM izdelane komponente dobro geometrijsko integriteto. Metalografska opazovanja so pokazala, da imajo komponente pretežno grobo dendritno morfologijo strjevanja s kontinuirno rastjo dendritov preko posameznih plasti nanašanja. Natezni preizkusi so pokazali minimalno anizotropijo natezne trdnosti. V smeri navarjanja je bila povprečna izmerjena natezna trdnost 148,7 MPa in vzporedno s smerjo navarjanja 146,1 MPa. Vendar pa je bil raztezek vzporedno s smerjo navarjanja občutno višji (23,91 %) kot v smeri pravokotno na navarjanje (19,31 %). Dobljeni rezultati za raztezek (od 19 do 24 %) precej presegajo vrednosti za konvencionalno litino 4043 (od 10 % do 15 %), verjetno zaradi manjše prisotnosti velikih livarskih napak (poroznost, votline nastale zaradi krčenja litine med ohlajevanjem). Rezultati te raziskave kažejo na velik potencial hibridne TIG-AM tehnologije za izdelavo komponent iz Al zlitin pri katerih se zahteva primerno razmerje med natezno trdnostjo in duktilnostjo.

Ključne besede: dodajalna tehnologija, proizvajanje zahtevnih izdelkov, aluminijeva zlitina tipa 4043, mikrostruktura po nanosu, mehanske lastnosti

1 INTRODUCTION

Additive manufacturing (AM), emerging in the 1980s, has evolved rapidly under various terminologies such as rapid prototyping, layered manufacturing, and freeform fabrication. While laser- and electron beam-based AM dominates metal processing, arc-based AM (e.g., TIG) offers cost-efficiency and high deposition rates, attracting growing interest. Prior studies highlight unique microstructural and mechanical characteristics in arc-deposited metals. For instance, Baufeld et al.[1] fabricated Ti-6Al-4V components via TIG AM, revealing anisotropic mechanical properties. Jiang et al.[2] reported higher tensile strength parallel to the welding direction in CMT-deposited 5356 aluminum alloy, while Skiba et al.[3] demonstrated that 308L stainless steel obtained via shaped metal deposition achieved tensile strengths comparable to conventional methods. Recent advancements in arc-based AM emphasize its potential for large-scale aluminum components due to reduced porosity and enhanced interlayer bonding.[4–6] However, challenges persist in controlling dendritic growth and mitigating hydrogen-induced defects in aluminum alloys.[7–9]

Therefore, this work investigates the microstructure and mechanical behavior of a TIG-deposited 4043 aluminum alloy, focusing on dendritic growth mechanisms and tensile anisotropy. The study builds on existing research to address critical gaps in understanding thermal history effects and hydrogen entrapment in arc-based AM processes.

2 EXPERIMENTAL PART

The TIG additive manufacturing system (**Figure 1**) employed a 3-axis gantry platform for precision spatial control, depositing an ER4043 aluminum alloy filler

*Corresponding author's e-mail:
28364524@qq.com (Lixing Qiu)

Figure 1: TIG additive manufacturing system

wire (1.2 mm diameter; **Table 1**) onto a 99.7 % pure aluminum substrate (200 × 100 × 4 mm) under 99.99 % argon shielding at 15 L/min. Critical process parameters (**Table 2**) comprised a 100 A welding current, 1650 mm/min wire feed rate, 500 mm/min travel speed, and 3 mm arc length, with Z-axis incremental lifting ensuring geometric consistency across layers. This protocol yielded rectangular and prismatic components with uniform 1.2 mm average layer thickness and 7.0 mm final wall dimensions (**Figure 3**). Post-fabrication evaluation involved transverse cross-sectional sampling perpendicular to the deposition path, segmented into three equidistant zones for metallographic analysis, complemented by tensile testing of horizontally (deposition-parallel) and vertically (build axis-aligned) oriented specimens conforming to **Figure 2** specifications.

We took one side of the aluminum alloy part and divided it into three roughly equal parts. We ground and polished its cross-section perpendicular to the weld and observed its microstructure. The microstructure corrosive solution used was 5 % HF. For the macrostructure, the corrosive solution used was HCl: HNO_3: HF = 75:25:5.

Table 1: Typical ER4043 chemical composition of the wire

Si	Mg	Fe	Cu	Al
5 %	≤0.10 %	≤0.04 %	≤0.05 %	balance

Table 2: Welding process parameters

Welding current (A)	100
Wire feed speed (mm/min)	1650
Welding speed (mm/min)	500
Arc length (mm)	3
Gas flow (L/min)	15

3 EXPERIMENTAL RESULTS AND DISCUSSION

3.1 Observation of the as-deposited microstructure

Macrostructure and microstructure analyses of three 4043 aluminum alloy specimens (labeled 1–3, from the topmost weld layer to the bottom layer), extracted from the central region of a bar-shaped component, from **Figure 4** revealed distinct layered characteristics.

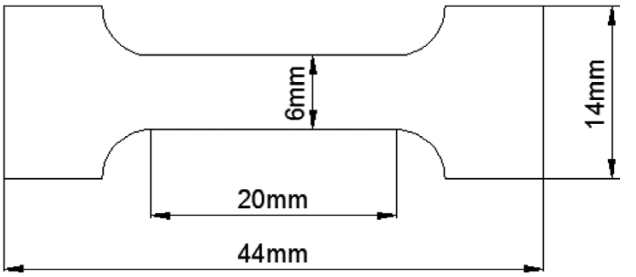

Figure 2: Dimensions of the tensile specimen

As shown in **Figure 4a**, Specimen 1 displays uniform and well-defined striations corresponding to weld layer fusion boundaries, with dendritic structures observed in the figure, exhibiting coarse columnar crystals (dendrite arm lengths of 600–800 μm), attributed to prolonged molten pool duration and slower cooling rates at the weld center. Specimen 2 (**Figure 4**b) demonstrates enhanced striation uniformity and clarity compared to

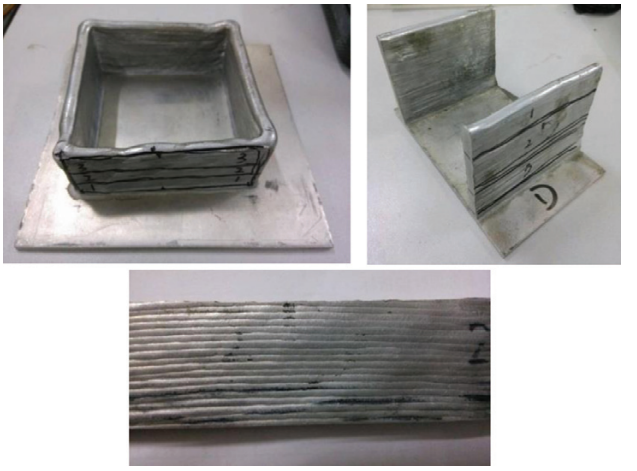

Figure 3: 4043 aluminum alloy square and strip parts: a) square parts, b) strip parts, c) side of the 4043 aluminum alloy part

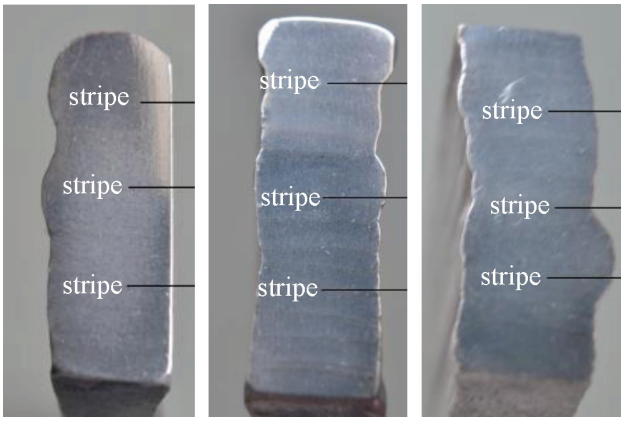

Figure 4: Micromorphology of specimens: a) Specimen 1, b) Specimen 2, c) Specimen 3

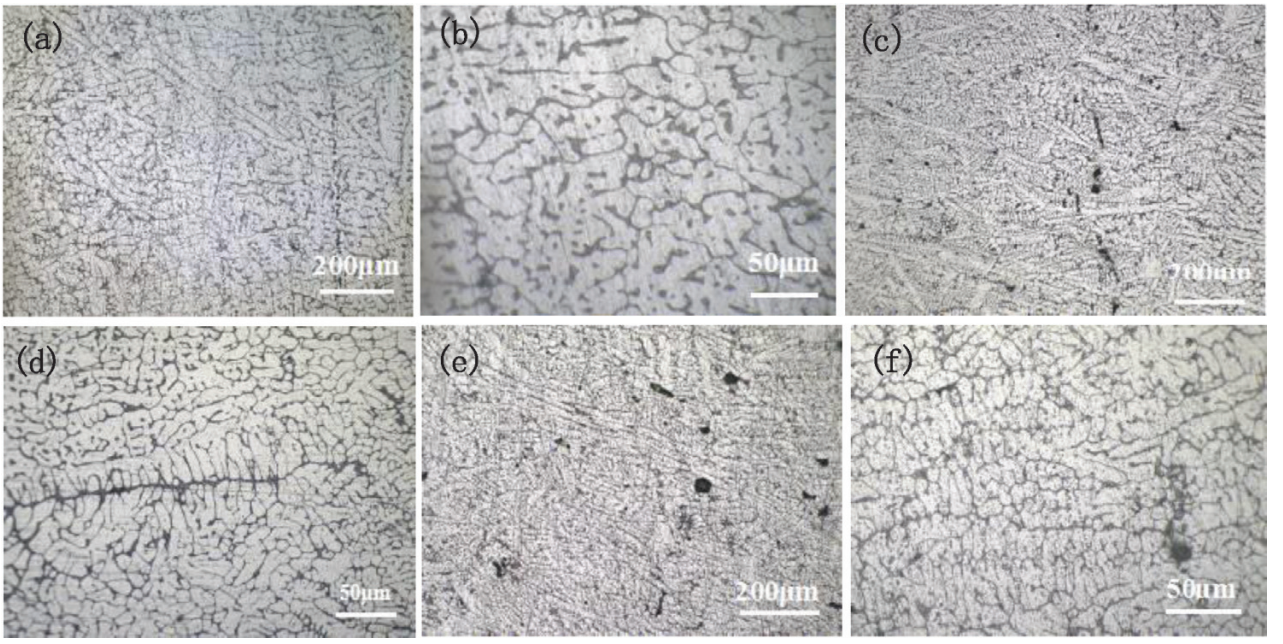

Figure 5: Microstructures of Specimens 1, 2 and 3 at different magnifications: a) and b) include Specimen 1; c) and d) include Specimen 2; e) and f) include Specimen 3

Specimen 1, though metallurgical examination in **Figures 5c** and **5d** reveals similar dendritic structures (600–800 μm arm lengths) with increased micropore density, suggesting incomplete hydrogen escape during solidification despite extended melt pool duration. Specimen 3 (**Figure 4c**) exhibits reduced striation consistency due to arc instability during weld initiation/termination, causing thickness variations, while **Figures 5e** and **5f** show elongated dendritic growth (500–800 μm arms) and hydrogen-induced porosity from substrate diffusion. Cross-sectional analysis confirms that all specimens contain parallel, equidistant bright striations representing sequential fusion layers, with columnar dendrites penetrating multiple layers and interdimeric eutectic formations. Notably, substrate-proximal Specimen 3 contains limited porosity. Weld orientation comparison in **Figures 6a–6c** demonstrates that weld-parallel sections contain fine equiaxed grains (0.5 mm visible pores in **Figure 6c**), while weld-perpendicular sections (**Figure 6d**) show slightly coarser but uniformly distributed equiaxed grains. Microstructural homogeneity across specimens indicates consistent thermal histories during multi-pass welding, with dendrite coarseness and porosity distribution governed by position-dependent cooling gradients and hydrogen diffusion kinetics from the pure aluminum substrate.

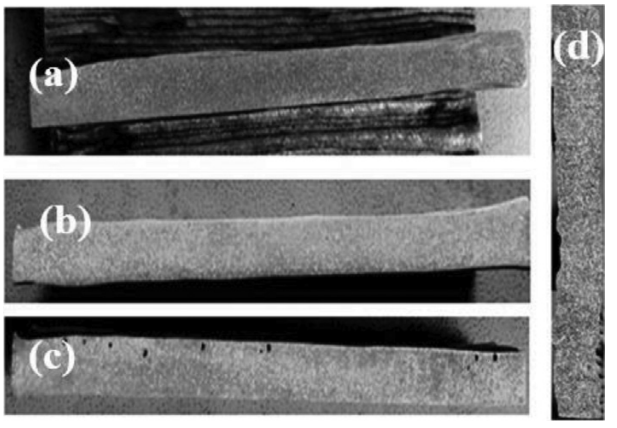

Figure 6: Macrostructure at different positions of the specimens

3.2 Mechanical properties

Tensile tests were conducted on three specimens aligned parallel to the weld direction and three specimens oriented perpendicular to the weld direction. The experimental data for the parallel orientation are presented in **Table 3**, while those for the perpendicular orientation are shown in **Table 4**. The average tensile strength of the 4043 aluminum alloy specimens tested parallel to the weld direction was 146.1 MPa, compared to 148.7 MPa for those tested perpendicular to the weld direction. The observed difference of 2.6 MPa between the two orientations falls within the range of potential experimental errors, indicating no statistically significant distinction in the tensile strength between the parallel and perpendicular orientations. Consequently, the tensile strength can be considered approximately equivalent across different loading directions. However, a notable discrepancy was observed in post-fracture elongation: the specimens tested parallel to the weld direction exhibited an average elongation of 23.91 %, whereas those tested perpendicular showed 13.31 % elongation, resulting in a substantial difference of 4.54 percentage points. This marked variation in elongation values demonstrates a directional dependence of ductility properties, suggest-

ing that the fracture elongation is orientation-sensitive despite the comparable tensile strengths. The results underscore the anisotropic mechanical behavior of the welded structure, where strength characteristics remain relatively isotropic while deformation capacity shows significant orientation-based differentiation.

Table 3: Tensile test parallel to the weld direction

No	Tensile strength (MPa)	Elongation (%)
1	147.8	23.34%
2	144.3	23.25%
3	146.2	24.13%
Average value	146.1	23.91%

Table 4: Tensile test perpendicular to the weld direction

No	Tensile strength (MPa)	Elongation (%)
1	145.9	18.87%
2	150.2	18.94%
3	149.6	20.13%
Average value	148.7	19.31%

Figure 7 shows hardness distribution curves for Specimens 1, 2 and 3 parallel to the weld direction from the arc striking position to the arc quenching position. It can be seen that the hardness of the specimens is high at the center; the average hardness of Specimen 3 (bottom) is high, while the average hardness of Specimen 1 (top) is low.

3.2 Disscussion

The coarse dendritic structure observed in the as-deposited 4043 aluminum alloy is a direct consequence of the high thermal input and slow cooling rates inherent to TIG additive manufacturing. The dendritic arm spacing (500–800 μm) aligns with typical observations in arc-based AM processes, where prolonged melt pool lifetimes promote unrestricted grain growth. The epitaxial growth of columnar dendrites across interlayer boundaries suggests a stable thermal gradient between successive layers. This phenomenon is critical in AM, as it reduces interfacial defects and enhances mechanical continuity. However, the coarsening of dendrites in the central region (**Figure 5b**) can be attributed to heat accumulation during multilayer deposition, which lowers the cooling rate and extends the time for grain boundary migration.

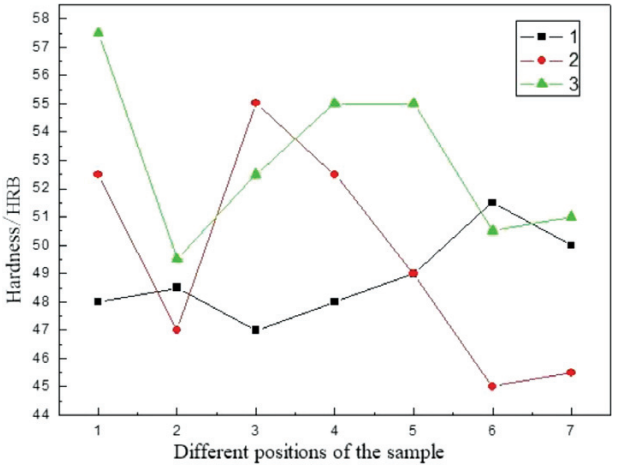

Figure 7: Hardness values at different positions of the samples

The localized porosity near the substrate (**Figure 6c**) is likely multifactorial. First, the pure aluminum substrate (99.7 % Al) contains trace impurities (e.g., Fe, Si) that may act as hydrogen traps. During welding, hydrogen from the substrate diffuses into the molten pool but fails to escape due to rapid solidification at the substrate interface. Second, the lack of preheating exacerbates thermal contraction stress, creating micro-voids. Mitigation strategies, such as substrate preheating or using a lower hydrogen-content base material, could reduce porosity. While the tensile strength anisotropy is minimal ($\Delta \approx 2.6$ MPa), the elongation disparity ($\Delta \approx 4.6$ %) reveals directional ductility differences. This can be dissected as follows: (1) Isotropic Strength: The near-uniform strength across orientations stems from the dominance of solid solution strengthening. Silicon (5 *w*/% in ER4043) dissolves into the aluminum matrix, creating lattice distortions that impede dislocation motion uniformly in all directions. The absence of deformation-induced textures (e.g., rolling or forging) further homogenizes strength. (2) Anisotropic Ductility: The higher elongation parallel to the welding direction (23.91 %) reflects the alignment of dendritic structures along the deposition path. Fracture preferentially propagates along inter-dendritic regions, which are less continuous perpendicular to the welding direction. Additionally, residual stresses from cyclic heating/cooling may constrain plastic deformation in the transverse direction, reducing elongation.

Each deposited layer subjects the underlying material to partial remelting and annealing, altering dislocation density and precipitation kinetics. This cyclic thermal history is a hallmark of AM processes and contributes to the hardness gradient. The tensile strength of TIG-deposited 4043 alloy (≈147 MPa) is lower than that of laser-based AM counterparts (e.g., ≈200 MPa for selective laser melted $AlSi_{10}Mg$), primarily due to coarser microstructures in arc-based processes. However, TIG AM excels in deposition efficiency (1650 mm/min wire feed vs. ≈10 g/h for laser AM), making it suitable for large-scale components where moderate strength suffices. The observed elongation (19–24 %) surpasses conventional cast 4043 alloys (10–15 %), likely due to the absence of large-scale casting defects (e.g., shrinkage cavities). This highlights the potential of TIG AM as a hybrid manufacturing method for aluminum components requiring balanced strength and ductility.

4 CONCLUSIONS

TIG-deposited 4043 aluminum exhibits a coarse dendritic microstructure with epitaxial growth across layers, influenced by thermal gradients and hydrogen entrapment.

Minimal tensile strength anisotropy (146–149 MPa) reflects uniform solid solution strengthening, while elongation anisotropy ($\Delta \approx 4.6\%$) arises from dendritic alignment and residual stresses. Hardness gradients are governed by microstructural coarsening and cyclic thermal history, offering avenues for property tailoring via process modulation.

The observed elongation (19–24 %) surpasses conventional cast 4043 alloys (10–15 %), likely due to the absence of large-scale casting defects (e.g., shrinkage cavities). This highlights the potential of TIG AM as a hybrid manufacturing method for aluminum components requiring balanced strength and ductility.

The hardness of the specimens is higher at the center, and the average hardness near the bottom of the substrate is higher, while the average hardness at the top is lower.

5 REFERENCES

[1] B. Bernd, B. Erhard, B. Omer, Wire based additive layer manufacturing: Comparison of microstructure and mechanical properties of Ti-6Al-4V components fabricated by laser-beam deposition and shaped metal deposition, Journal of Materials Processing Tech., 211 (**2011**) 6, 1146–1158, doi:10.1016/j.jmatprotec.2011.01.018

[2] Y. Jiang, J. Zhang, C. Xu, et al., Research on aluminum alloy rapid forming technology and process based on cold metal transfer, J. Mater. Sci. Technol., 31 (**2015**) 3, 255–263, doi:10.1016/j.jmst.2014.11.020

[3] T. Skiba, B. Baufeld, O. Van der Biest, Microstructure and mechanical properties of stainless steel component manufactured by shaped metal deposition, ISIJ Int., 49 (**2009**) 10, 1588–1591, doi:10.2355/isijinternational.49.1588

[4] D. Ding, Z. Pan, D. Cuiuri, et al., A multi-bead overlapping model for robotic wire and arc additive manufacturing (WAAM), Robot. Comput. Integr. Manuf., 31 (**2015**) C, 101–110, doi:10.1016/j.rcim.2014.08.008

[5] J. Guo, Y. Zhou, C. Liu, et al., Wire arc additive manufacturing of AZ31 magnesium alloy: Grain refinement and mechanical properties, Mater. Sci. Eng. A, 772 (**2020**), 138697, doi:10.1016/j.msea.2019.138697

[6] W. Wang, X. Li, Z. Hou, et al., Study on the microstructure and properties of AZ31 magnesium alloy alternating pulse TIG welding, Sci. Technol. Vis., 36 (**2019**), 72–74, doi:10.19619/j.issn.1007-3723.2019.36.022

[7] J. Zhang, H. Li, Y. Liu, et al., Hydrogen porosity in TIG-welded aluminum alloys: Mechanisms and mitigation, J. Mater. Process. Technol., 240 (**2017**), 320–327, doi:10.1016/j.jmatprotec.2016.10.022

[8] S. W. Williams, F. Martina, A. C. Addison, et al., Wire + Arc additive manufacturing, Mater. Sci. Technol., 32 (**2016**) 7, 641–647, doi:10.1179/1743284715Y.0000000107

[9] P. A. Colegrove, H. E. Coules, J. Fairman, et al., Microstructure and residual stress improvement in wire and arc additively manufactured parts through high-pressure rolling, J. Mater. Process. Technol., 213 (**2013**) 10, 1782–1791, doi:10.1016/j.jmatprotec.2013.04.012